Journal for ImmunoTherapy of Cancer

Potent and durable control of mesothelin-expressing tumors by a novel T cell-secreted bi-specific engager

Paris Kosti,[1] Johan Abram-Saliba,[1] Laetitia Pericou-Troquier,[1] Sarah Pavelot,[1] Tiphaine Ruggeri,[1] Marc Laffaille,[1] Melita Irving ,[1] George Coukos,[1,2] Evripidis Lanitis ,[1] Steven M. Dunn [1,2]

To cite: Kosti P, Abram-Saliba J, Pericou-Troquier L, *et al*. Potent and durable control of mesothelin-expressing tumors by a novel T cell-secreted bi-specific engager. *Journal for ImmunoTherapy of Cancer* 2025;**13**:e010063. doi:10.1136/jitc-2024-010063

► Additional supplemental material is published online only. To view, please visit the journal online (https://doi.org/10.1136/jitc-2024-010063).

EL and SMD contributed equally.

Accepted 23 February 2025

[1]Department of Oncology, Ludwig Cancer Research Lausanne Branch, University of Lausanne, Lausanne, Switzerland
[2]Department of Oncology, CHUV, Lausanne, Switzerland

Correspondence to
Dr Steven M. Dunn;
steven.dunn@chuv.ch

ABSTRACT

Background The glycosylphosphatidylinositol-anchored cell surface protein mesothelin (MSLN) shows elevated expression in many malignancies and is an established clinical-stage target for antibody-directed therapeutic strategies. Of these, the harnessing of autologous patient T cells via engineered anti-MSLN chimeric antigen receptors (CAR-T) is an approach garnering considerable interest. Although generally shown to target tumor MSLN safely, CAR-T trials have failed to deliver the impressive curative or response metrics achieved for hematological malignancies using the same technology. A need exists, therefore, for improved anti-MSLN molecules and/or more optimal ways to leverage immune effector cells.

Methods We performed ELISA, label-free kinetic binding assays, FACS, Western blotting, and transient recombinant MSLN expression to characterize the recognition properties of a novel CAR-active human scFv clone, LABC-13F08. To investigate T cell redirection, we conducted kinetic IncuCyte co-culture killing assays using transduced primary T cells and MSLN$^+$ target cell lines and assessed levels of activation markers and effector cytokines. The antitumor potential of LABC-13F08 formatted as a bispecific engager (BiTE) was evaluated in vivo using transduced human primary T cells and immunocompromised NSG mice xenografted with ovarian, mesothelioma, and pancreatic MSLN$^+$ tumor cell lines.

Results The LABC-13F08 scFv is highly unusual and distinct from existing (pre)clinical anti-MSLN antibody fragments, exhibiting an absolute requirement for divalent cations to drive MSLN recognition. As a monovalent BiTE, LABC-13F08 demonstrates robust in vitro potency. Additionally, primary human T cells engineered for constitutive secretion of the 13F08 BiTE exhibit strong antitumor activity toward in vivo ovarian and mesothelioma xenograft models and show encouraging levels of monotherapy control in a challenging pancreatic model. LABC-13F08 BiTE secreted from engineered T cells (BiTE-T) can both recruit non-engineered bystander T cells and also induce activation-dependent MSLN-independent bystander killing of cells lacking cognate antigen. To address safety concerns, 13F08 BiTE-T cells can be rapidly targeted for clearance via a molecular "off" switch.

Conclusions The novel LABC-13F08 scFv exhibits a mode of binding to MSLN which is not observed in typical anti-MSLN antibodies. Efficacious targeting by a T cell secreted engager would represent a clinically differentiated approach for the treatment of MSLN$^+$ tumors.

WHAT IS ALREADY KNOWN ON THIS TOPIC

⇒ Preclinical and clinical evidence indicates that mesothelin (MSLN), a tumor-associated antigen showing a broad and robust distribution across different cancers, can be safely targeted via antibody-based immunotherapeutic T cell recruitment/redirection.

WHAT THIS STUDY ADDS

⇒ A T cell-secreted bispecific engager comprising a novel, fully human, and differentiated anti-MSLN scFv warhead can specifically and potently redirect T cells to attack solid tumors. In contrast to chimeric antigen receptor T cell (CAR-T) formats, this can potentially amplify tumor destruction through the recruitment of large numbers of tumor-proximal bystander T cells.

HOW THIS STUDY MIGHT AFFECT RESEARCH, PRACTICE OR POLICY

⇒ The combination of a new "fit-for-purpose" bispecific T cell engager employed in a secretory adoptive cell therapy context represents an unexplored approach for the clinical treatment of diverse MSLN-positive tumors.

INTRODUCTION

The redirecting of patient autologous effector T cells to attack malignant tumors, independently of any natural cognate recognition mediated through TCR-pMHC interactions, is now an established therapeutic paradigm, with both chimeric antigen receptor (CAR-T) and soluble bispecific engager (BiTE®, Amgen trademark; hereafter BiTE) technologies having revolutionized the treatment of certain blood cancers. For solid tumors, however, these approaches have met with only limited clinical success. In addition to several "immune escape" mechanisms comprising various physical and immunosuppressive chemical barriers that actively exclude and/

or dysregulate tumor-targeting lymphocytes,[1] solid tumors typically lack public surface antigens that are completely absent from critical healthy tissues. Nevertheless, significant over-expression of certain tumor-specific and tumor microenvironment-associated antigens (TAAs), together with the presence of disease-related neo-epitopes, splice-isoforms, and conformers, can provide adequate targeting differentiation and opportunities for therapeutic intervention, as can approaches specifically tailored to tumor physiology.[2–5]

One such TAA of active clinical interest, the differentiation antigen mesothelin (MSLN), is a post-translationally processed, glycosylphosphatidylinositol (GPI)-anchored cell surface-bound protein, whose normal physiological expression is limited and restricted to the mesothelial cells of the pleura, pericardium, and peritoneum, with trace amounts reported in a limited set of additional tissues.[6 7] MSLN was originally identified in human ovarian carcinoma cells[6] and has subsequently been found to be overexpressed in many diverse cancers, including malignant mesothelioma, (triple-negative) breast cancers, ovarian carcinomas, pancreatic cancer, and pediatric acute myeloid leukemia, among others.[7–11] Increased MSLN expression has typically been associated with a poorer prognosis for patients across multiple tumor indications.[9 12–14] As of January 2025, ClinicalTrials.gov reports ~130 interventional NCT studies targeting MSLN expressed in tumors, with the majority (~56%) involving engineered CAR- or TCR-based adoptive cell therapy (ACT) strategies, with or without the incorporation of soluble molecule cotherapy. Interestingly, the soluble T cell CD3 engager class is represented by only three single phase 1/2 studies (NCT06756035; NCT06255665; NCT03872206). To date, although demonstrating encouraging safety and tolerance data, clinical trials of anti-MSLN CAR-T products have shown only limited efficacy as monotherapies, with no studies having yet progressed beyond phase 2.

Mature, processed MSLN is a 40 kDa protein with the majority of its structure shown to comprise a predominantly super-helical solenoid arrangement with armadillo-like repeats defining a series of three stacked regions or domains.[15] The N-terminal region is suggested to be the most immunogenic, least flexible part of the structure, hosting recognition sites for several key clinical antibodies, in addition to the heavily glycosylated cell adhesion mucin, CA-125, which can co-occur as a prognostic factor in MSLN$^+$ tumors.[16] The C-terminal region of MSLN contains the GPI-anchor transamidation signal motif together with several exposed labile peptide bonds in the juxta-membrane sequence that are substrates for certain proteases capable of shedding the MSLN into the tumor stroma and serum of patients.[17] Truncated splice-isoform(s) also contribute to this circulating pool of MSLN, which may reach concentrations sufficient to act as a decoy ligand for anti-MSLN therapeutics.[18] The function of MSLN under normal physiological conditions remains unclear, although KO models and its GPI-linkage support its involvement in tumor cell adhesion, migration, and metastasis.[19] Little is known about how native, GPI-anchored MSLN is organized at the cell surface, or how GPI moieties may directly or indirectly influence its conformation, although studies suggest that the removal of GPI moieties—and the lipid interactions they mediate—from certain membrane proteins can perturb distant epitopes recognized by antibody reagents.[20]

The anti-MSLN antibody fragments currently exploited for (pre)clinical CARs and/or immunotoxins have typically emerged via immunization or in vitro affinity-driven display technologies and share the characteristic of strong binding to recombinant MSLN or its soluble fragments, possessing KDs in the pM to double-digit nM range.[21–31] Previously, we used a simple "affinity-blind" phenotypic library selection and screening approach to isolate a panel of fully human scFv clones based solely on a surrogate CAR reporter read-out. One such molecule, LABC-13F08 exhibited promising in vitro CAR effector activity toward MSLN$^+$ cognate target cells yet, unexpectedly, showed negligible binding to recombinant MSLN using standard assays.[32] We, thus, sought to investigate in parallel (1) the apparently contradictory and atypical biochemical behavior of 13F08 relative to other reported anti-MSLN scFvs and (2) how it might be leveraged as a component of an internal clinical ACT program.

MATERIALS AND METHODS

All materials and experimental methods, including a key resources table, are detailed in online supplemental methods.

RESULTS

LABC13F08 exhibits atypical, context-sensitive binding to MSLN

Functional CAR activity requires the physical bridging of a CAR scFv with target antigen on a tumor cell. We thus sought to understand the discordance in our previous LABC-13F08 scFv (hereafter 13F08) data which demonstrated compelling CAR activation toward MSLN$^+$ cells in the absence of appreciable in vitro binding to soluble recombinant (r) human (h) MSLN. Convenient monovalent (BiTE) and dimeric bivalent forms of 13F08 (Fc-fusion) were thus produced and purified from transiently transfected HEK293-6E cells, and their binding properties were variously compared with reference to representative clinical and preclinical comparator molecules, including SS1, M5, 15B6, P4, and MH1.[21 23 24 27 33] Initially, we performed kinetic biolayer interferometry (BLI) against immobilized high-quality, C-terminally biotinylated rhMSLN. In contrast to SS1, a clinically validated CAR-active scFv included as a positive control, the 13F08-BiTE bound weakly, with extended association-phase data indicating a monomer KD in the µM range (online supplemental figure S1a–d). Similarly, titration ELISA data revealed weak binding of the bivalent 13F08-Fc

relative to representative comparator anti-MSLN Fc-fusions, and also no cross-reactivity with biotinylated recombinant murine MSLN (online supplemental figure S1e,f).

Despite the apparent poor recognition of rhMSLN by 13F08, we reasoned that it must stain MSLN$^+$ cell lines in order to account for the previously observed activity of the 13F08 scFv CAR. We thus used FACS to profile the binding of 13F08-Fc against a panel of endogenous MSLN$^+$ tumor and negative control cell lines. Here, we also included clinical (SS1, M5) and preclinical (15B6) CAR-active binders as Fc-fusion comparators, as well as the original anti-MSLN reference mAb, K1.[6] Although substantial differences in median MFI staining signals were evident across the different lines, likely reflecting distinct MSLN epitope exposure/accessibility environments (a consequence of differences in PTM profiles and/or possible masking due to cis-acting ligands), 13F08-Fc selectively recognized the six tested MSLN$^+$ cells, although with smaller MFI shifts for HeLa and OVCAR3. For SKOV3, heterogeneous staining was evident by logarithmic FACS histogram consistent with the K1 reference staining (figure 1A,B). Further, we confirmed a significant correlation in target cell staining between 13F08 and the K1 reference (figure 1C). Western blot analysis performed on solubilized whole cell extracts of these lines mirrored this FACS data, confirming the ability of 13F08-Fc to specifically recognize endogenous native MSLN (online supplemental figure S2). In this study, we also observed specific Western staining of MSLN from extracts of HEK293-6E suspension cells transfected with both the major (ISO#2) and minor (ISO#1) full-length (FL) GPI-anchored MSLN transcript variants (mature, processed ORFs) and a truncated fragment comprizing the two N-terminal domains (D1-D2), but not of various other domain fragments (online supplemental figure S3a,b). Additionally, 13F08-Fc could also immuno-precipitate FL-MSLN from solubilized cells in

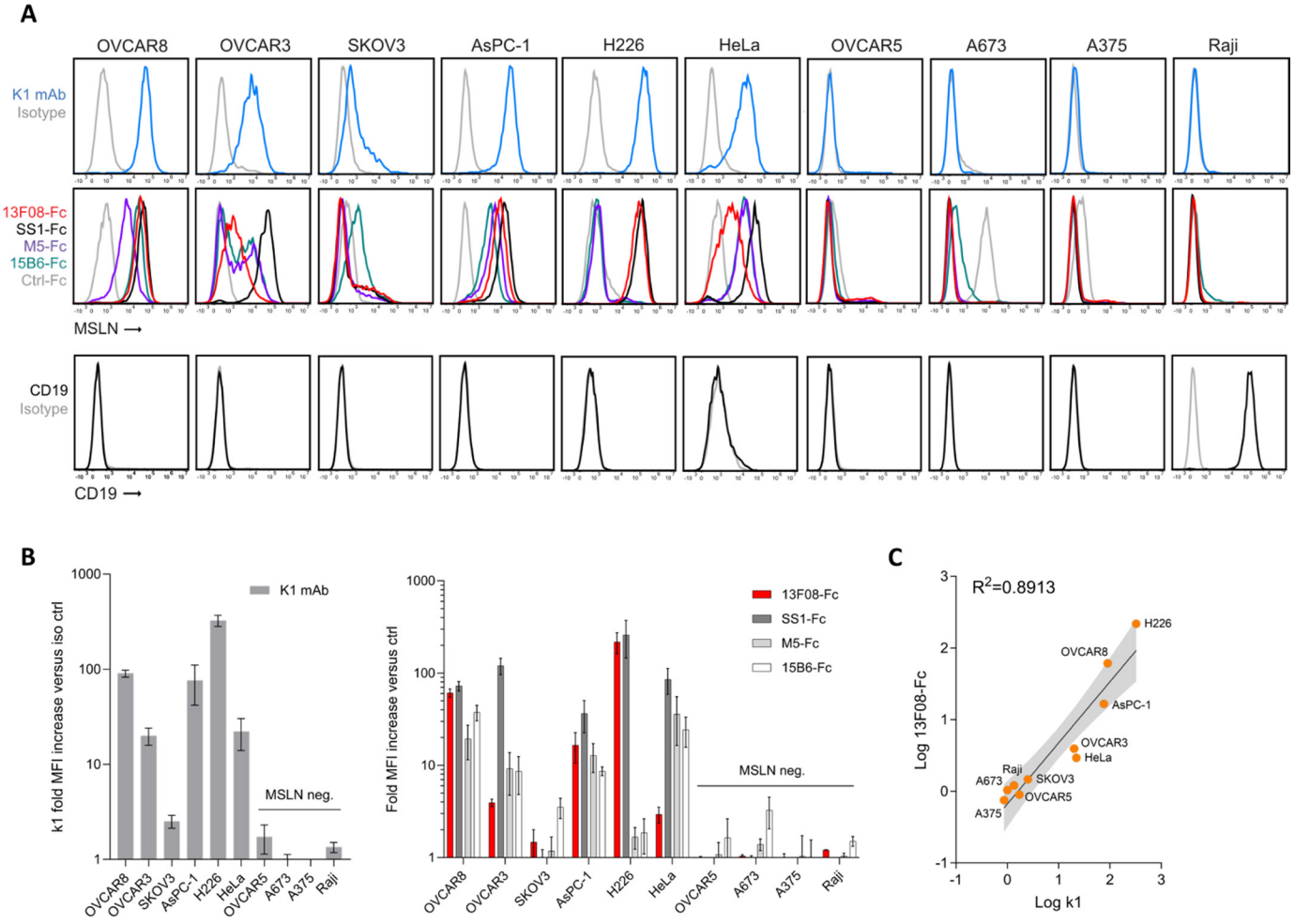

Figure 1 (A) Logarithmic FACS staining of MSLN$^+$ and negative endogenous cell lines. Staining was performed using 2 µg/mL for both mAb K1 (upper panels; isotype ctrl at matched concentration) and the individual Fc-fusions (middle panels; Ctrl-Fc was anti-TEM1 which stains A673 TEM1$^+$/MSLN-neg control cells). CD19 staining (lower panels) was performed to assess the expression of CD19 on the indicated cell lines; Raji were used as a positive control for CD19 staining. All data normalized to mode. (B) Median fluorescence intensity (MFI) FACS profiling of K1 mAb (left), and 13F08-Fc and comparators (right; all at 2 µg/mL) versus MSLN$^+$ and negative control tumor cell lines. Data derived using FACS buffer comprising PBS/2% FBS. (C) Correlation plot of MSLN expression detected by K1 mAb versus 13F08-Fc binding (fold MFI increase over ctrl) in different cell lines. Data plotted are the means±SEM from n=2–4 independent experiments. FBS, fetal bovine serum; MSLN, mesothelin.

this recombinant system (online supplemental figure S4). Of note, commercial rhMSLN included as a lane marker in these immune-blotting experiments was also readily stained by 13F08-Fc, which was unexpected in light of our ELISA/BLI findings. A further discrepancy was highlighted by FACS profiling of MSLN-transfected HEK293-6E cells. Here, in contrast to the strong staining observed toward certain endogenous MSLN$^+$ tumor lines (H226, OVCAR8, AspC-1), 13F08-Fc stained transfected HEKs only partially and exhibited significantly lower staining sensitivity than seen for representative comparator Fc-fusions (online supplemental figure S5a). Confirming the above WB observations, only transfected FL-MSLN and the D1-D2 truncated fragment gave convincing MFI shifts (online supplemental figure S5b). Interestingly, this partial staining behavior was retained for a chimeric D1-D2 fragment when human D1 was fused to murine D2 but not for the vice versa arrangement. As expected, fully murine D1-D2 expressed in HEKs was not recognized by 13F08 (online supplemental figure S5b). All comparators gave the expected fragment recognition profiles in accordance with the published literature.

The binding of LABC-13F08 to MSLN has an absolute requirement for divalent cations

To elucidate these contextual inconsistencies in MSLN recognition by 13F08, we asked whether an explanation could be found in the different buffer and/or media systems employed in the various assays. Indeed, we established that strong apparent binding of 13F08 correlated only with the inclusion of potentially rich sources of metal cations in the experiment (milk as a blocking reagent in WB and IP; FBS routinely included in the FACS buffer when staining tumor lines). Thus, in our above ELISA/BLI experiments, the free metal availability would be low and restricted to ions passively associated with the purified BSA used as a blocking reagent and diluent carrier. Similarly, the suspension HEK293-6E cells used for FL-MSLN (and fragment) transfections were cultured in serum-free medium, with FACS analysis conducted in buffers including an excess of the strong chelator, EDTA.

Subsequently, we revisited our binding assays, conducting them in the presence or absence of exogenously added metals or EDTA, and confirmed a striking requirement for divalent cations in the interaction of 13F08 with purified rhMSLN protein, MSLN-transfected HEK293-6E cells, and endogenous MSLN$^+$ OVCAR8 cells (figure 2, online supplemental figures S6 and S7). Several metals were shown to promote strong monophasic binding, with this dependency only evident for 13F08 and not the anti-MSLN comparators examined. Kinetic BLI measurements performed in the presence of 1 mM $CaCl_2$ indicated a monomer KD toward rhMSLN in the region of 9 nM, whereas EDTA inclusion in the buffer completely ablated residual binding (figure 2C). Interestingly, substitution of the native MSLN GPI-anchor motif with the type I TM domain of human HER2 in our transfection FACS assay appeared to ablate the partial biphasic staining when EDTA was included in the staining buffer, whereas in the absence of EDTA (and in the presence of 2% FBS), this variant was stained strongly (online supplemental figure S7).

Collectively, our MSLN truncation and chimeric fragment data indicate that the epitope recognized by 13F08 resides within the D1-D2 fragment, is insensitive to the presence of the minor transcript (ISO#1) D2 splice insertion, does not involve the N-glycon in the D1-D2 linker, and that binding to both FL-MSLN and D1-D2 is strongly facilitated by divalent metal cations present at high levels in serum and milk (online supplemental figure S7).[34 35] Thus, 13F08 represents a novel anti-MSLN antibody which is distinguished from other reported molecules by its unusual recruitment of metal to enable single-digit nM KD target binding.

LABC-13F08 efficiently mobilizes T cells as a purified BiTE

As LABC-13F08 was originally isolated from a functional CAR screen, we next asked whether this T cell redirection property also extended to the scFv BiTE format. We expressed and purified a panel of several promising scFv candidates (emerging from both our CAR phenotypic and classical phage display screens) as soluble scFv1(αMSLN)-scFv2(αCD3ε) BiTEs and screened their capacity in vitro to trigger effector activity against MSLN$^+$ tumor lines in co-cultures containing primary T cells. Unexpectedly, 13F08 appeared to be the most potent of the tested BiTEs in an IncuCyte kinetic cell killing assay, specifically driving clearance of OVCAR8, H226, and SKOV3 cognate target cells, inducing IFN-γ secretion, and activating an NFAT reporter Jurkat cell line in the presence of both hMSLN-transfected HEKs and endogenously expressing OVCAR8 cells (figure 3A and online supplemental figure S8). Interestingly, we observed that certain comparator CAR scFvs exhibited similarly compelling in vitro efficacy in the purified BiTE format. Here, SS1, M5, and 15B6 compared favorably with 13F08 in their control of OVCAR8 and SKOV3 target cells (figure 3B).

T cells engineered to constitutively secrete LABC-13F08 monovalent BiTE show specific and potent in vitro activity toward MSLN$^+$ tumor lines

Intrigued by our findings, we next asked whether human T cells could be engineered to secrete active 13F08 BiTE at levels sufficient to drive efficient T cell redirection in the presence of cognate target cells. To confirm the translation/expression potential of a codon-optimized version of the 13F08 scFv in primary human T cells, we first confirmed its expected functional behavior as a second-generation 4-1BBζ CAR (online supplemental figure S9). Subsequently, we engineered T cells to express a secreted FLAG-tagged 13F08-BiTE (figure 4A). We applied imaging flow cytometry to confirm the presence of a functional CD3ε-interacting BiTE (online supplemental figure S10a), and flow cytometry to confirm binding of T cell-secreted 13F08-BiTE to native tumor cell-expressed MSLN (online supplemental figure S10b).

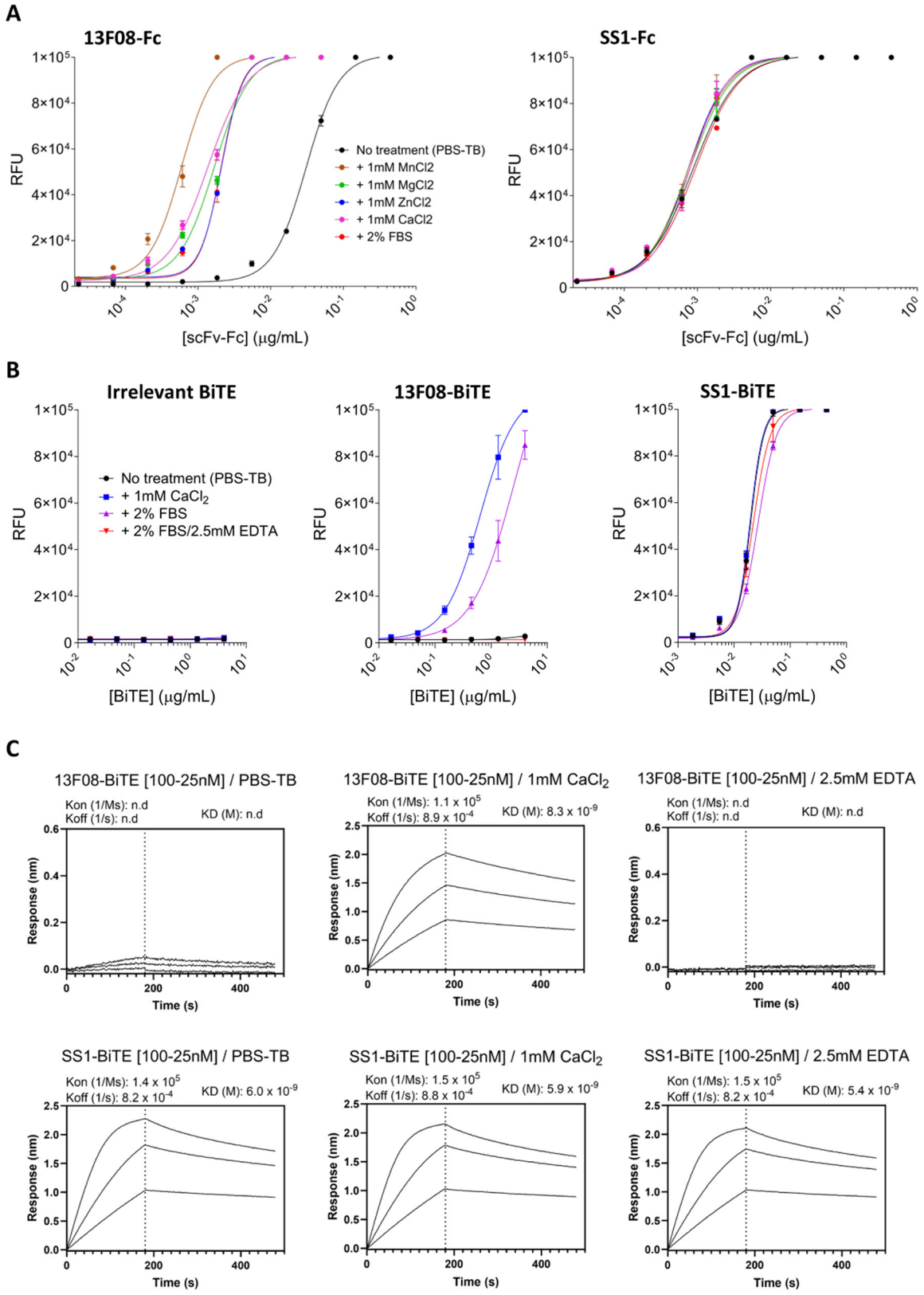

Figure 2 Impact of divalent cations on the recognition of MSLN by 13F08. (A) Titration ELISA demonstrating the behavior of bivalent 13F08-Fc and SS1-Fc against biotinylated recombinant hMSLN in the presence of exogenously added metals or FBS. (B) Titration ELISA data showing the binding of purified monovalent 13F08-BiTE to biotinylated human MSLN relative to the representative SS1-BiTE comparator when excess metal cations are available (1 mM $CaCl_2$ and 2% FBS) or sequestered (2% FBS+2.5 mM EDTA). Data are shown as the mean of n=3 technical replicates±SEM. (C) Kinetic biolayer interferometry sensorgrams for purified 13F08-BiTE and SS1-BiTE binding to immobilized biotinylated human MSLN in the presence or absence of $CaCl_2$. FBS, fetal bovine serum; MSLN, mesothelin.

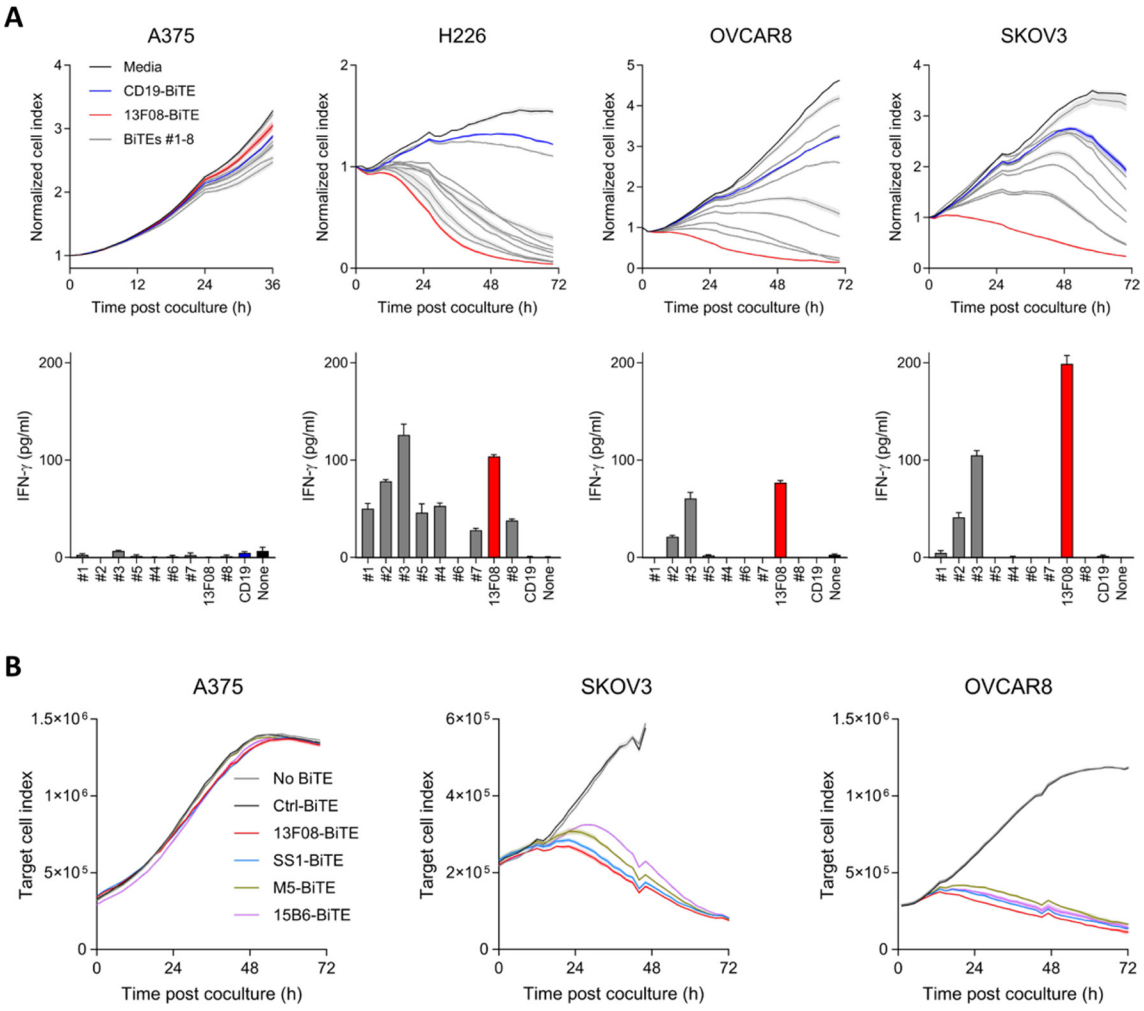

Figure 3 Evaluation of purified soluble BiTEs for activity in co-cultures of primary human T cells and target tumor cell lines. (A) Representative IncuCyte screening assays showing kinetic killing profiles for three endogenous MSLN$^+$ tumor lines obtained with a panel of purified BiTEs, including 13F08 (upper panels), with associated secretion of IFNγ (lower panels). (B) Evaluation of 13F08-BiTE alongside other anti-MSLN scFvs derived from established CARs and formatted as BiTEs (data shown are from donor-matched T cells and are representative of n=4 T cell donors). Data curves and shading indicate mean±SEM, respectively (n=3 technical replicates); BiTEs were used at a final concentration of 4 nM with an E:T ratio of 2:1 for both (A) and (B); A375 was included as a MSLN-negative control line. E:T, effector-to-target; MSLN, mesothelin.

Importantly, we also observed that the 13F08-BiTE T cells (hereafter, BiTE-T) predominantly exhibited a T_{cm} phenotype (induced by our T cell expansion protocol) that was indistinguishable from that of non-transduced (NT) T cells as indicated by positivity for the discriminating CD45RO, CCR7, CD28, and CD27 T_{cm} markers (online supplemental figure S11a). Additionally, 13F08 BiTE-T cells do not show any significant cytokine release nor upregulation of tonic signaling markers relative to the NT or CD19 CAR-engineered T cell backgrounds (online supplemental figure S11b,c).

We next performed kinetic IncuCyte assays to assess the extent of any specific target cell killing. Encouragingly, the growth curves of all MSLN$^+$ tumor lines, including SKOV3, which is stained only modestly with 13F08-Fc, were efficiently suppressed by the 13F08 BiTE-T cells, indicating that secreted BiTE concentrations rapidly achieve levels that exceed activation thresholds in these cultures (figure 4A,B). Notably, the A673 and OVCAR5 MSLN-negative control lines were completely spared, with negligible secretion of effector cytokines or induction of activation markers on the T cells in these cultures (figure 4C). Additionally, the induction of typical activation markers and certain effector cytokines in 13F08 BiTE-T co-cultures was seen to correlate with the levels of tumor cell surface MSLN as determined by the commercial K1 reference mAb (figure 4D and online supplemental figure S12). We next confirmed the binding of T cell-secreted BiTEs to NT T cells (figure 5A,B) and asked whether BiTE-T secreted 13F08 BiTE could function in trans to recruit NT bystander T cells to mediate killing of cognate MSLN$^+$ target cells. We observed that a single supplementation with 13F08 BiTE-T cell media is sufficient to robustly redirect non-engineered T cells to kill MSLN$^+$ targets and to trigger effector cytokine secretion (figure 5C,D). Additionally, we also titrated the

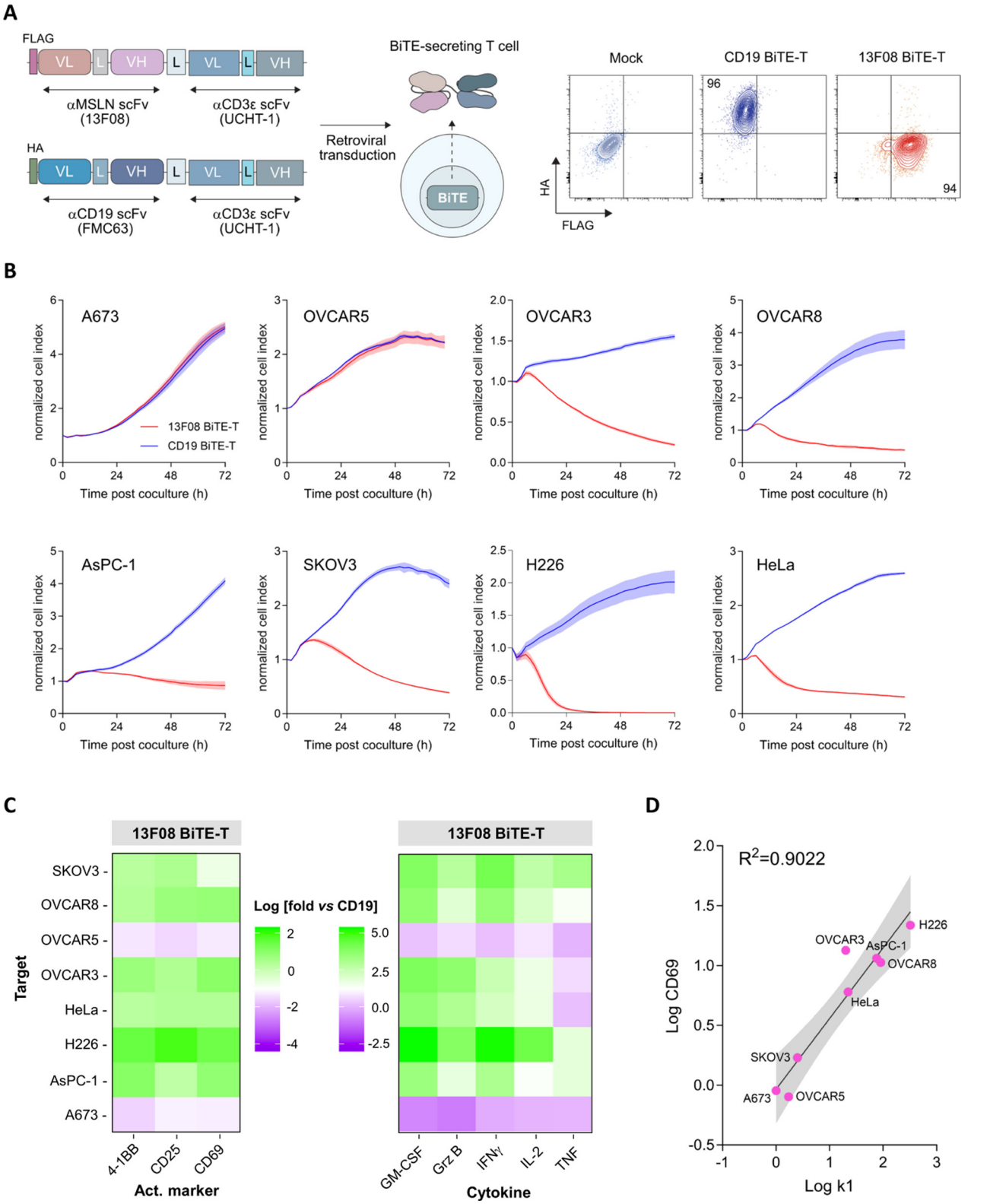

Figure 4 Target cell killing mediated by 13F08 BiTE-T secretor effector cells. (A) Schematic illustrating secretory retroviral BiTE constructs (left) with transduction efficiencies determined by FACS (right). (B) IncuCyte kinetic cytotoxicity co-culture assays showing specific and potent killing by 13F08 BiTE-T cells of MSLN$^+$ tumor lines while sparing the MSLN-negative control lines (A673 and OVCAR5). (C) Heat maps depicting profiles and relative magnitudes of upregulated activation markers and effector cytokines for the co-cultures in (B). Data depicted as fold-difference relative to the CD19 BiTE-T controls after 24 hours of co-culture. Assays conducted at an effector-to-target (E:T) ratio of 2:1. (D) Correlation plot of CD69 expression versus K1 mAb FACS staining in different cell lines. Data in (B–D) obtained with donor-matched T cells. Representative data shown. Experiments were repeated with T cells from at least n=3 donors with similar results. Data curves and shading in (B) indicate mean±SEM. MSLN, mesothelin.

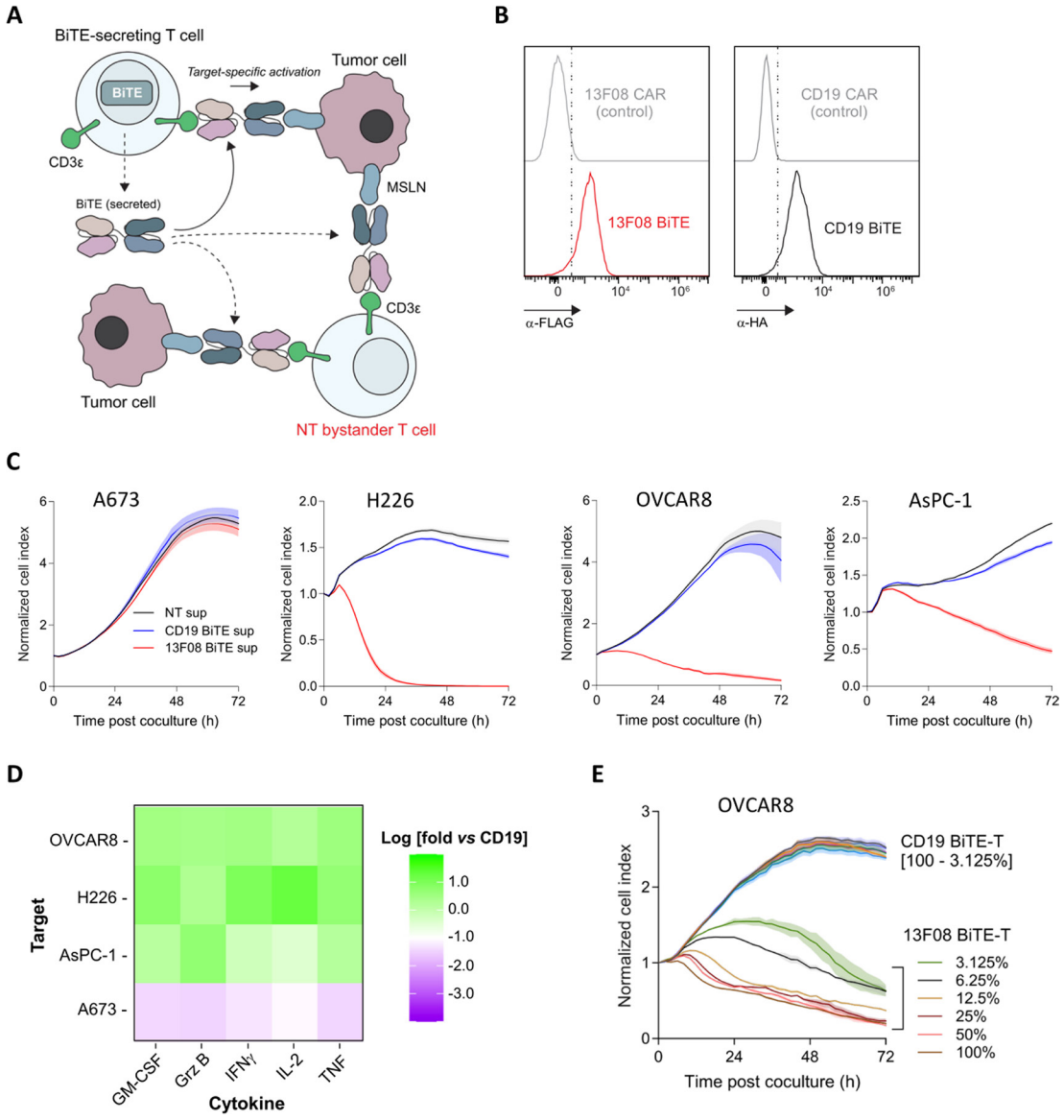

Figure 5 13F08 BiTE-T can potently prime functional killing of cognate MSLN$^+$ target cells by non-transduced (NT) bystander T cells. (A) Schematic illustration of potential mechanisms of bystander T cell recruitment by secreted BiTE. (B) Secreted 13F08-BiTEs and CD19-BiTEs in BiTE-T cell media can stain CD3ε on NT T cells. BiTE constructs as illustrated in figure 4A. (C) NT T cell redirected killing of co-cultured MSLN$^+$ tumor lines by a single addition of 13F08 BiTE-containing culture media supernatant from engineered T cells. A673 cells were used as a MSLN-negative control. (D) Heat map depicting effector cytokine upregulation (post-24 hours of co-culture) of 13F08 BiTE-activated NT cells in the presence of MSLN$^+$ tumor lines versus the A673 MSLN-negative control. (E) IncuCyte cytotoxicity co-culture titration assay. Engineered BiTE-T (>75% transduction efficiency) are combined at the indicated percentage with NT donor-matched T cells (to give a fixed cell count of 100% total cells). Total T cell:target ratio in (C–E) maintained at 2:1 for all conditions. Data curves and shading indicate mean±SEM, respectively (n=3 technical triplicates). Experiments in (B–E) were repeated independently at least twice with T cells from at least n=2 donors. Representative data are shown. MSLN, mesothelin.

percentage composition of 13F08 BiTE-T cells present in the bulk effector cell population at a standard 2:1 effector to target ratio. Strikingly, we observed substantial control of OVCAR8 MSLN$^+$ cells with as few as 3% of the effectors arising from the 13F08 BiTE-T preparation (figure 5E). Notably, the real-time killing kinetics also suggested a lag at low BiTE-T cell numbers, likely indicating an accumulation phase whereby secreted BiTE levels gradually attain the necessary threshold concentrations required for subsequent widespread T cell recruitment and effector activation (figure 5E).

Finally, we asked how 13F08 BiTE-T cell in vitro efficacy would compare with 13F08 CAR-T (4-1BBζ) cells against OVCAR8, H226, and AsPC-1 cells. Here, we used a suboptimal E:T ratio of 1:1 with high cell transduction efficiencies (~80% for both BiTE and CAR). We observed that 13F08 BiTE-secreting T cells exhibited rapid and robust target cell killing kinetics, particularly toward H226, when

compared alongside their 13F08 CAR-T counterparts. The increased apparent potency exhibited by the 13F08 BiTE-T cell format correlated with target-specific cytokine release profiles that were more robust and uniform than those seen for the CAR (online supplemental figure S13). We speculate that the profound recruitment of potentially all T cells present in the co-culture (including NT, as highlighted in figure 5), together with the activation signal proceeding through engagement of the

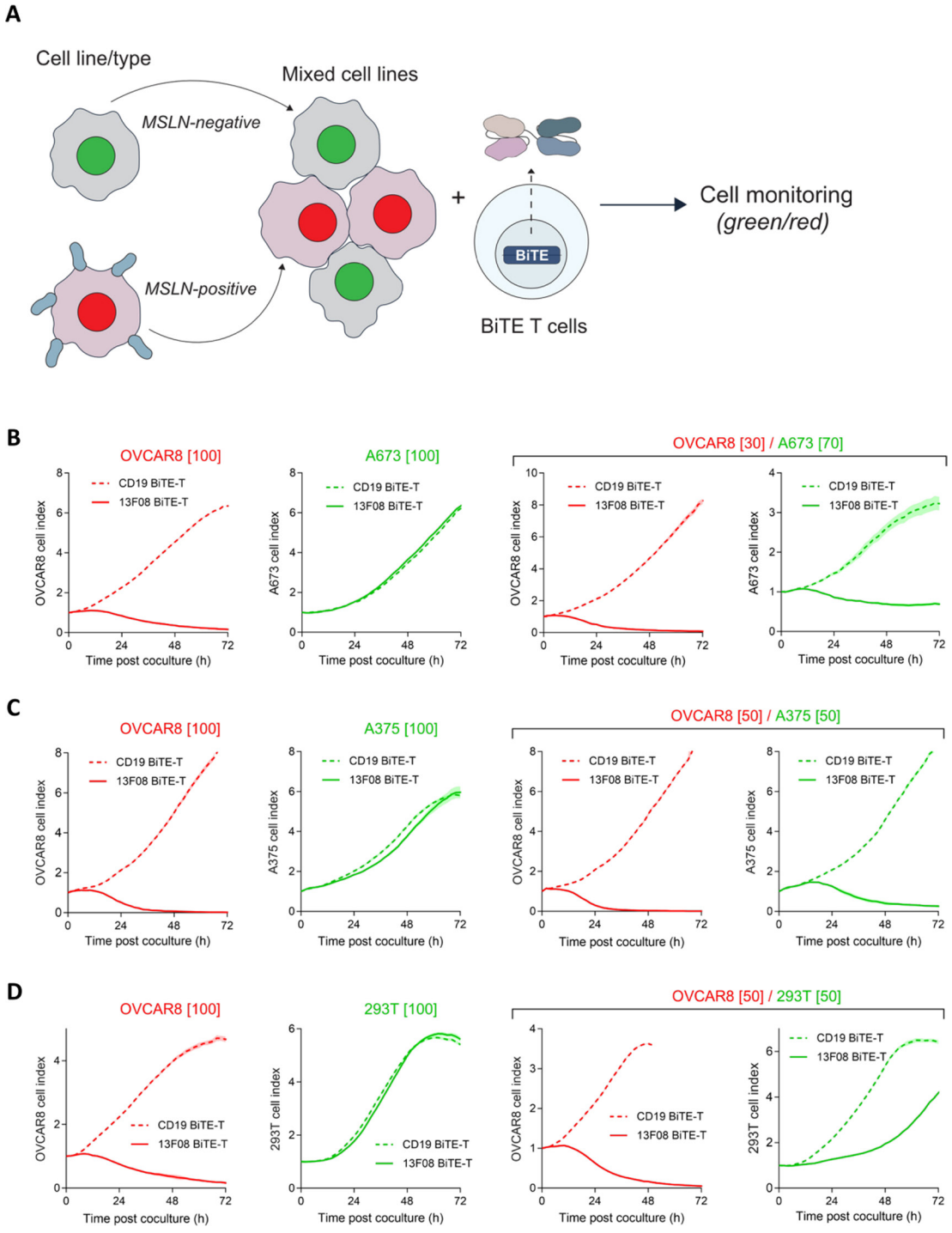

Figure 6 13F08 BiTE-T bystander cell killing. (A) Schematic illustration of triple co-culture assay set up. (B-D) Bystander impact on MSLN-negative cells (A673, A375, HEK293T) by 13F08 BiTE-T cells activated specifically in the presence of cognate MSLN$^+$ OVCAR8. OVCAR8 and MSLN-negative tumor cells were differentially labeled for individual fate tracking as shown in (A) and combined according to the proportions indicated in parentheses to correct for their relative in vitro proliferation rates. Data curves and shading indicate mean±SEM, respectively (n=3 technical triplicates). Experiments were repeated independently at least twice with T cells from at least n=2 donors. Representative data are shown. Assays conducted at an effector-to-target (E:T) ratio of 2:1. MSLN, mesothelin.

sensitive native CD3/TCR complex likely accounts for the observed performance of 13F08 BiTE-T.

13F08 BiTE-T cells demonstrate both MSLN$^+$ target cell-dependent bystander killing in vitro and exhibit insensitivity to soluble MSLN decoy fragments

The localized "bystander" killing of adjacent non-cognate target cells by pre-activated CD8$^+$ cytotoxic T cells has been previously described,[27 36] and strategies to induce or stimulate this activity to augment the efficacy of CAR-T therapies toward solid tumors are areas of active investigation.[37] Interestingly, significant in vitro killing of MSLN-negative bystander cells was previously reported during the characterization of the P4 anti-MSLN CAR.[27] In an IncuCyte assay comprising co-cultures of cognate MSLN$^+$ OVCAR8 cells and A673 or A375 tumor cells lacking MSLN, we observed robust killing of both A673 and A375 cells by 13F08 BiTE-T cells only in the presence of MSLN$^+$ OVCAR8 cells, which was not due to soluble factors present in the OVCAR8 culture supernatant (figure 6A–C and online supplemental figure S14a). This would imply the activation of a pathway—or pathways—associated with the engagement of death receptors (e.g., FAS or DR5) on A673 and A375 cells. Interestingly, in co-cultures containing the non-tumor HEK293T cell line, bystander killing by activated 13F08 BiTE-T was not observed, although the growth of the HEKs was significantly slowed (figure 6D). Future studies will be required to elucidate these data. We also asked whether 13F08 BiTE-T killing efficacy could be impacted by the presence of soluble "decoy" MSLN fragments shed from tumor cells by cell surface protease activity.[17] We observed no apparent inhibition of OVCAR8 killing kinetics when native, shed MSLN from spent and concentrated OVCAR8 supernatants (160 ng/mL final concentration) was included in the assay. Similarly, 1.3 µg/mL of commercial, purified rhMSLN was also without effect (online supplemental figure S14b).

LABC-13F08 BiTE-secreting T cells show potent in vivo antitumor activity in ACT xenograft models

We next performed an in vivo study in which we treated established subcutaneous OVCAR8 tumors in immunodeficient NSG mice with two cycles of intravenously infused high-dose 13F08 BiTE-T (figure 7A). Notably, we observed complete tumor eradication by 13F08 BiTE-T monotherapy with no outward signs of toxicity (online supplemental figure S15). Additionally, we also analyzed tumor tissue from mice cohorts treated in parallel at an advanced stage of tumor control (once tumor volumes had decreased to ~22 mm^3). Tumors from those mice treated with 13F08 BiTE-T cells showed not only strikingly higher levels of infiltration by the CD45$^+$ ACT product than the CD19 BiTE control tumors but also elevated Ki-67 expression, suggestive of a higher proliferative capacity of these cells in response to MSLN-driven antigen encounter (figure 7B). 13F08 BiTE-T ACT cell levels determined at this time point for peripheral blood were similarly higher than those observed for the CD19 control. Extending the study, we challenged 13F08 BiTE-T cells against xenografted H226 and SKOV3 tumors, observing a rapid clearance of the former following ACT (figure 7C). In our previous profiling experiments, SKOV3 cells exhibited weak and heterogeneous anti-MSLN staining, with low anti-MSLN WB sensitivity (figure 1 and online supplemental figure S2). Nevertheless, 13F08 BiTE-T cells achieved an impressive level of tumor control, with outgrowth only resuming approximately 10 days after ACT. We speculate that the escape of SKOV3 xenograft tumors may be due to the survival of a pre-existing compartment of cells expressing levels of MSLN beneath the threshold for functional 13F08-BiTE control. We cannot, however, exclude inefficient bystander killing as a contributory factor, either due to weaker T cell activation generally (due to lower MSLN antigen density), or to the absence of compatible death receptors on SKOV3.

To better evaluate the in vivo potency of 13F08 BiTE-T cells, we performed two further experiments using lower dose ACT T cell regimens. Encouragingly, two ACT cycles comprising a total of 18×10^6 BiTE-T cells were sufficient to eradicate OVCAR8 tumors (figure 7D). Interestingly, ex vivo analysis of peripheral blood T cell counts 1 week post-tumor clearance revealed the presence of only a few surviving cells, suggesting only limited capacity for survival in the absence of ongoing tumor stimulation. In a further experiment, we generated an additional xenograft model using AsPC-1, an aggressive pancreatic tumor line known to be difficult to control in the xenograft setting.[38] We treated mice bearing established AsPC-1 tumors with a single low dose of 10×10^6 13F08 BiTE-T cells and observed a significant tumor growth arrest. Ex vivo analysis confirmed a strong infiltration and activation of T cells relative to the CD19 BiTE-T control treatment and, as for OVCAR8, a low T cell presence in the peripheral blood (figure 7E). The low persistence of the ACT product in the circulation observed for these two distinct NSG models also explains the absence of any obvious GvHD in these experiments. Consistent with this, for all in vivo models, we observed no indications of peripheral toxicity as assessed by the monitoring of animal behavior, weight, and survival over the period of the study (online supplemental figure S15).

As a negative in vivo control to further confirm the specificity of 13F08 BiTE-T cells, mice were implanted with OVCAR5, a line that profiles as either negative or very low for MSLN expression by FACS staining (figure 1 and online supplemental figure S2).[27] As expected, OVCAR5 tumors were not controlled by 13F08 BiTE-T cells (online supplemental figure S16).

LABC13F08 BiTE-secreting T cells can be rapidly cleared using a truncated EGFR safety switch

The absence of observable toxicity in our NSG xenograft models following the systemic ACT of constitutively expressing 13F08 BiTE-T cells provides confidence that this novel scFv does not exhibit any obvious off-target or

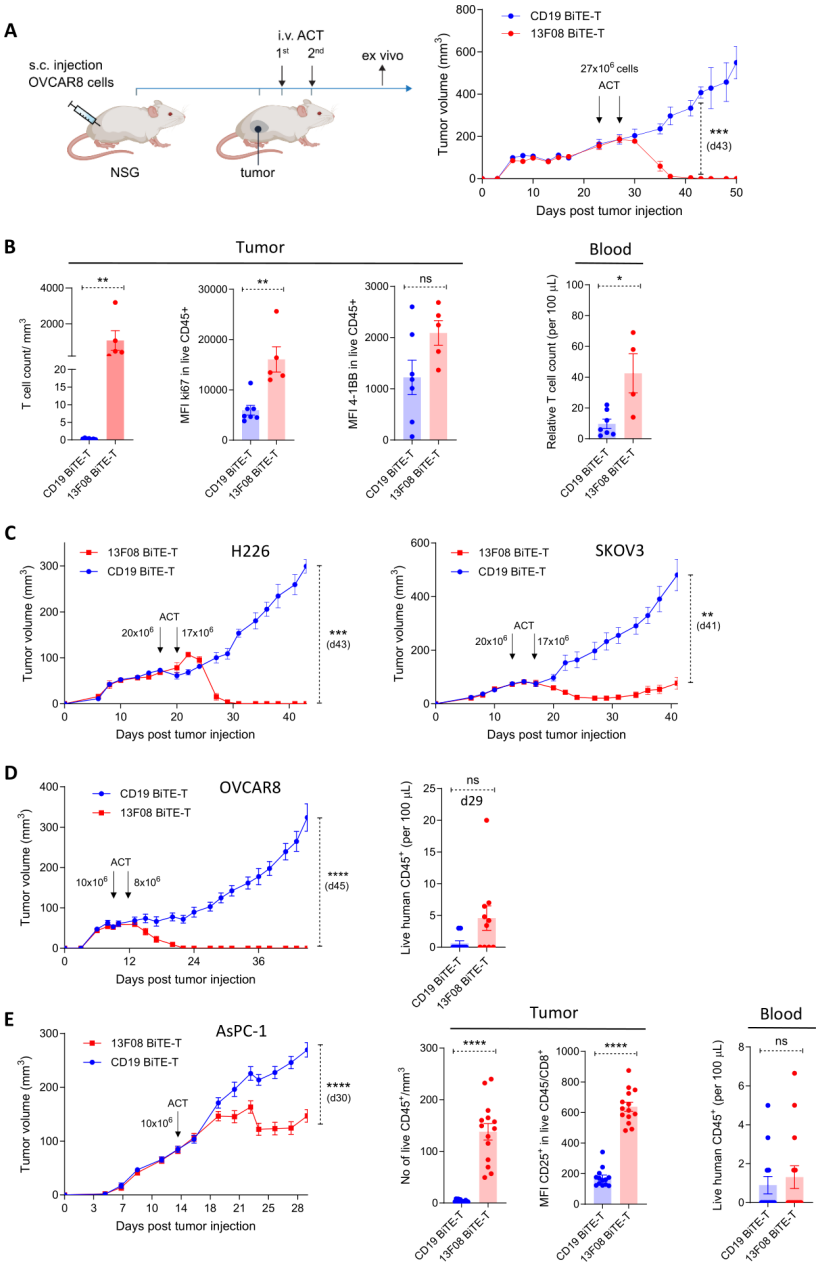

Figure 7 In vivo antitumor efficacy of adoptivelytransferred 13F08 BiTE-T cells in NSG mice. (A) Schematic of experimental format for the OVCAR8 xenograft model (left) with comparative tumor progression curves in mice treated with two high doses (27×10^6 per dose) of ACT product (right). Significance test: two-way ANOVA with Sidak correction, curve analysis post ACT1 until d43 (n=6 per group); ***p=0.0002. (B) Ex vivo profiling of preclearance residual OVCAR8 tumors (sampled when ~22 mm^3) from (A) in a replicate experiment (n=7 per group). Tumor-infiltrating ACT T cell count in tumors from mice with the indicated treatment and their expression of Ki67 and 4-1BB proliferation and activation markers, respectively, determined by FACS analysis (data point drop-outs were due to complete tumor clearance at the time of sampling, hence no material available). ACT T cell count in peripheral blood of mice treated with the indicated treatment (per 100 µL; data point drop-outs were due to sample coagulation). Significance test: two-tailed Mann-Whitney; ns, not significant; *p<0.05, **p<0.01, ***p<0.001. (C) Progression curves for H226 (n=5 per group) and SKOV3 (n=6 per group) tumor xenografts. Significance tests: two-way ANOVA with Sidak correction; **p<0.01, ***p<0.001. (D) Tumor progression curves for an OVCAR8 xenograft model treated with a reduced total ACT cell dose (n=10 per group, left). Significance test: Repeated measures ANOVA with Sidak correction; ****p<0.0001. ACT T cell count in peripheral blood from mice treated as indicated (right). Blood was analyzed (per 100 µL) on d29 (~1 week post-tumor clearance in the 13F08 BiTE-T group). Significance test: unpaired, two-tailed t-test; ns, not significant. (E) Tumor progression curves for an AspC-1 xenograft model (n=13–14 per group) treated with a single reduced ACT dose (left). Significance test: two-way repeated measures ANOVA with Sidak correction; ****p<0.0001. Ex vivo profiling of T cell-infiltrated tumors at d30 (right). Tumor-infiltrating T cell count and CD25 late activation marker expression on ACT T cells determined by FACS. ACT T cell count in peripheral blood (per 100 µL) from mice that have received the indicated treatment. Significance tests: unpaired, two-tailed t-test. Data are presented as mean±SEM; CD19 BiTE-T as irrelevant control. Corresponding animal weight curves are shown in online supplemental figure S15. ACT, adoptive T cell transfer; ANOVA, analysis of variance.

"sticky" behavior when challenged with the plethora of naturally occurring murine cell-surface tissue antigens. As 13F08 does not recognize native murine MSLN or, by inference, those healthy somatic mouse tissues that express low endogenous target levels, these models cannot inform on the risk of possible on-target-off-tumor toxicity when translating to the human setting. Hence, we considered it prudent to investigate a mechanism to ablate adoptively-transferred 13F08 BiTE-T cells to further mitigate clinical risk. One such strategy is the coexpression of a truncated non-signaling EGFR (tEGFR) which retains the depleting epitope recognized by the FDA-approved antibody drug, Cetuximab.[39] We, therefore, re-engineered our BiTE-T vector with an upstream tEGFR sequence appended for coexpression via a P2A sequence (online supplemental figure S17a,b). Encouragingly, in vitro co-culture IncuCyte killing experiments revealed no impact of the coexpressed tEGFR on target cell killing kinetics, or on the secretion of the effector molecules IFN-γ and Granzyme B, relative to the singly-engineered 13F08 BiTE-T cells (online supplemental figure S17c). We next asked whether cetuximab-mediated clearance could operate in vivo using an NSG xenograft model. Although lacking NK cells, immune compartments potentially capable of eliciting ADCC/P (eg, macrophages, neutrophils) are still present in these mice. We treated OVCAR8 tumor-bearing mice with two ACT cycles using co-engineered tEGFR/13F08 or tEGFR/CD19 BiTE-T cells. One day following each ACT, mice were treated with cetuximab or rituximab control antibody and monitored for tumor growth (online supplemental figure S17d). Importantly, we observed that administration of cetuximab, but not rituximab, resulted in a total cessation of tumor control by dual-engineered tEGFR/13F08 BiTE-T cells. Additionally, these dual-engineered BiTE-T cells and their respective antibody treatments induced no apparent toxicity in the mice (online supplemental figure S17e). Hence, our data suggest that rapid depletion of the 13F08 BiTE engineered T cell population postinfusion using the tEGFR system is feasible and efficient and may merit consideration in a clinical setting.

DISCUSSION

CAR-T or soluble T cell engagers offer great potential as toolkit components for the treatment of solid tumors, not least due to their sensitivity and effector-driven amplification potential. For either approach, it can be argued that the requisite targeting scFvs (or equivalent fragments) should ideally derive from tailored, bottom-up screening programs with these specific applications as the primary focus. In phenotypic reporter-enrichment experiments, we previously identified LABC-13F08, a fully human "fit-for-purpose" anti-MSLN scFv capable of driving productive cell-bridging and strong signal transduction as a generic second-generation CAR.

In the current study, we report three key findings. First, 13F08 retains potent and selective T cell redirection activity when reformatted, expressed, and purified as a classical tandem BiTE with a humanized anti-CD3ε scFv. We have observed previously that molecules emerging from our CAR screen may be predisposed to such dual functionality, which is likely due to common requirements for a permissive bridging distance and geometry between the epitope and T cell surface, together with an intrinsic minimal monovalent affinity requirement for registering in our CAR reporter assay.

Second, we identify an unusual, absolute requirement for divalent metal cations in the interaction of 13F08 with hMSLN. None of the comparator molecules we evaluated exhibited this requirement, and to the best of our knowledge, no studies implicating metal coordination in the binding of any other anti-MSLN antibody fragment or known natural ligand have been described. Additionally, no bound metal ion adduct is evident in the few reported MSLN crystal structures. This would argue against a metal-induced conformational shift within MSLN that creates/exposes an epitope for 13F08 and would instead favor a model of an atomic coordination shell that is exclusively derived from sequence features within the 13F08 CDRs or that is shared between MSLN and the scFv. Interfacial metal ion involvement in antibody recognition is rare, with only a few examples reported—all of which use Ca^{2+} to either form an electrostatic "bridge" to the antigen or to stabilize a particular paratope conformation.[40–42] Interestingly, in our BLI kinetic affinity experiments, Ca^{2+} was seen to promote the greatest affinity gain, bringing the effective monovalent KD of 13F08 into the single-digit nM range, which is sufficient to account for its observed soluble BiTE activity. As the concentration of accessible Ca^{2+} in the extracellular milieu of the tumor microenvironment is considered to be in excess of 1 mM, the level of this cofactor is unlikely to be limiting for optimal 13F08 function in vivo. Ongoing structural and biochemical studies will aim to further elucidate the details of this novel MSLN-Ca^{2+}-antibody binding interaction.

Finally, we were interested to explore whether our 13F08 BiTE could have potential utility in ACT as a T cell secreted antitumor agent. The secreted BiTE-T conceptual paradigm is gaining traction as an alternative or partner strategy to CAR-T. To date, several studies have reported encouraging preclinical proof-of-concept data using secreted BiTEs targeting several distinct TAAs including CD123, EGFR, EphA2, Frα, FAP, EGFRvIII, and IL13Rα2 tumor antigens, either as single agents or paired with a cotransduced second BiTE or a CAR.[43–48] Recently, a dual EGFRvIII-CAR/EGFR-BiTE approach was the subject of a glioblastoma clinical trial report.[49] Collectively, this body of data suggests that leveraging the potency of the BiTE drug format in a BiTE-T ACT setting has great potential. To counter a rapid clearance due to their small size and lack of an Fc domain, tandem soluble BiTE drugs are clinically administered by continuous infusion, which is associated with narrow therapeutic windows and non-specific systemic toxicities.[50] By contrast, infused BiTE-T cells, which retain the potential to persist and

expand, can traffic to tumor sites where they can deliver locally active concentrations of BiTE. Interestingly, at least two studies using different tumor xenograft mouse models have shown that, following ACT, secreted BiTE levels in the peripheral blood remain below the thresholds of detection.[44 45] This raises the intriguing question of whether constitutively expressing BiTE-T cell reagents may possess a clinical safety advantage over soluble BiTE drugs. One may speculate that intrinsically lower levels of mRNA and constitutive protein expression in unstimulated BiTE-T cells could work in concert with renal and pharmacological clearance mechanisms to resist the accumulation of secreted BiTE in the systemic circulation. Following trafficking to the tumor and extravasation, basal levels of secreted BiTE appear sufficient to activate BiTE-T producer cells in the presence of tumor antigen. The resulting upregulation of BiTE-T global protein expression could, in principle, lead to increased BiTE secretion at the tumor site and bystander recruitment within the TME.[45]

To the best of our knowledge, our data represent the first demonstration that a MSLN-targeting BiTE-T reagent can efficiently control endogenous MSLN$^+$ tumor cells both in vitro and in vivo. Further, our data indicate that 13F08 BiTE-T cells exhibit or promote target cell-dependent bystander killing and show no functional sensitivity to shed or soluble MSLN fragments. Additionally, we observe that 13F08 BiTE-T cells can be rapidly ablated in vivo using a commercial antibody-based safety "switch". Previous BiTE-T studies have all enlisted existing "off-the-shelf" rodent/humanized mAbs which have been reverse-engineered into scFvs for BiTE construction. In contrast, 13F08 represents the first reported BiTE-T fully human scFv warhead isolated de novo as a functional CAR/BiTE.

As a stand-alone monotherapy, 13F08 BiTE-T persistence and proliferation in the clinical setting could be a concern due to the absence of adequate costimulatory signaling. This has been raised by others who observed significant checkpoint expression and a loss of memory and naïve BiTE-T cell phenotypes following prolonged antigen stimulation in a mouse model.[48] Currently, it is unknown if chronically stimulated, non-proliferating BiTE-T cells could persist within a malignancy and retain competency as bio-reactors, continuing to secrete active levels of diffusible BiTE. If this is the case, one may speculate that local bystander TILs, phenotypically diverse and lacking the signatures of chronic antigen stimulation, could still be effectively recruited for tumor control. Studies to explore this scenario, together with the further augmentation of 13F08 BiTE-T performance through coengineering with additional effector and/or signaling components for persistence and expansion are ongoing.

CONCLUSIONS

The data in this manuscript describe LABC-13F08, a novel metal-dependent human anti-MSLN scFv, and demonstrate for the first time that a BiTE-T cell strategy can be leveraged to control and even eliminate different endogenous MSLN$^+$ tumor cells both in vitro and in vivo. Conceptually, this presents a significantly differentiated approach to current anti-MSLN CAR-T ACT, with 13F08 BiTE-T providing a potent and diffusible active amplification agent capable of engaging both producer and bystander T cells via the native CD3/TCR complex.

Acknowledgments The authors would like to thank Jean-François Mayol and the UNIL FACS facility for excellent FACS support and guidance, Kevin Lau from the Protein Production and Structure Core Facility (EPFL) for assistance with the GatorPrime, and the Animal facility of the University of Lausanne. We would also like to thank Rachid Lani, Sheuli Begum, and Bili Seijo for molecular biology support and Greta Giordano-Attianese, Mélanie Triboulet, Bovannak Chap, Miruna Burdjula, Giulia Fonti, and Jennifer Murray for help with experiments. Kirsten Scholten and members of the Irving lab contributed to helpful discussions, and Gerd Ritter assisted with critical reading of the manuscript.

Contributors SMD, EL and PK contributed to conceptualization, methodology, validation, formal analysis, resources, writing, review and editing, visualization, supervision and project administration. JA-S contributed to methodology, data acquisition, formal analysis, visualization and writing. SP, TR, LP-T and ML were involved in methodology and data acquisition. GC contributed to conceptualization, project administration, review and editing. MI contributed resources and project administration. SMD and EL are responsible for the overall content. The guarantor of the study is SMD.

Funding This work was supported by Ludwig Cancer Research (to SMD, LAbCore), the Fondazione Teofilo Rossi di Montelera e di Premuda (administered by the Carigest Foundation), and the Swiss National Science Foundation (SNSF 310030_204326 to MI).

Competing interests None declared.

Patient consent for publication Not applicable.

Ethics approval All in vivo studies were approved and conducted in accordance with the Service of Consumer and Veterinary Affairs of the Canton of Vaud (Cantonal authorization: VD3887b) and Swiss federal law (National authorization: 35774).

Provenance and peer review Not commissioned; externally peer reviewed.

Data availability statement All data relevant to the study are included in the article or uploaded as supplementary information.

ORCID iDs
Melita Irving http://orcid.org/0000-0002-6849-7194
Evripidis Lanitis http://orcid.org/0000-0002-8194-5414
Steven M. Dunn http://orcid.org/0000-0002-7402-9581

REFERENCES

1 Labani-Motlagh A, Ashja-Mahdavi M, Loskog A. The Tumor Microenvironment: A Milieu Hindering and Obstructing Antitumor Immune Responses. *Front Immunol* 2020;11:940.
2 Haen SP, Löffler MW, Rammensee H-G, *et al*. Towards new horizons: characterization, classification and implications of the tumour antigenic repertoire. *Nat Rev Clin Oncol* 2020;17:595–610.

3 Andersen MH. Tumor microenvironment antigens. *Semin Immunopathol* 2023;45:253–64.
4 Garrett TPJ, Burgess AW, Gan HK, *et al*. Antibodies specifically targeting a locally misfolded region of tumor associated EGFR. *Proc Natl Acad Sci U S A* 2009;106:5082–7.
5 Kosti P, Opzoomer JW, Larios-Martinez KI, *et al*. Hypoxia-sensing CAR T cells provide safety and efficacy in treating solid tumors. *Cell Rep Med* 2021;2:100227.
6 Chang K, Pastan I, Willingham MC. Isolation and characterization of a monoclonal antibody, K1, reactive with ovarian cancers and normal mesothelium. *Int J Cancer* 1992;50:373–81.
7 Chang K, Pastan I. Molecular cloning of mesothelin, a differentiation antigen present on mesothelium, mesotheliomas, and ovarian cancers. *Proc Natl Acad Sci U S A* 1996;93:136–40.
8 Weidemann S, Gagelmann P, Gorbokon N, *et al*. Mesothelin Expression in Human Tumors: A Tissue Microarray Study on 12,679 Tumors. *Biomedicines* 2021;9:397.
9 Cheng W-F, Huang C-Y, Chang M-C, *et al*. High mesothelin correlates with chemoresistance and poor survival in epithelial ovarian carcinoma. *Br J Cancer* 2009;100:1144–53.
10 Le K, Wang J, Zhang T, *et al*. Overexpression of Mesothelin in Pancreatic Ductal Adenocarcinoma (PDAC). *Int J Med Sci* 2020;17:422–7.
11 Kaeding AJ, Barwe SP, Gopalakrishnapillai A, *et al*. Mesothelin is a novel cell surface disease marker and potential therapeutic target in acute myeloid leukemia. *Blood Adv* 2021;5:2350–61.
12 Inoue S, Tsunoda T, Riku M, *et al*. Diffuse mesothelin expression leads to worse prognosis through enhanced cellular proliferation in colorectal cancer. *Oncol Lett* 2020;19:1741–50.
13 Feng F, Zhang H, Zhang Y, *et al*. Level of mesothelin expression can indicate the prognosis of malignant pleural mesothelioma. *Transl Cancer Res* 2020;9:7479–85.
14 Suzuki T, Yamagishi Y, Einama T, *et al*. Membrane mesothelin expression positivity is associated with poor clinical outcome of luminal-type breast cancer. *Oncol Lett* 2020;20:193.
15 Zhan J, Lin D, Watson N, *et al*. Structures of Cancer Antigen Mesothelin and Its Complexes with Therapeutic Antibodies. *Cancer Res Commun* 2023;3:175–91.
16 Chen S-H, Hung W-C, Wang P, *et al*. Mesothelin binding to CA125/MUC16 promotes pancreatic cancer cell motility and invasion via MMP-7 activation. *Sci Rep* 2013;3:1870.
17 Liu X, Chan A, Tai C-H, *et al*. Multiple proteases are involved in mesothelin shedding by cancer cells. *Commun Biol* 2020;3:728.
18 Zhang Y, Chertov O, Zhang J, *et al*. Cytotoxic Activity of Immunotoxin SS1P Is Modulated by TACE-Dependent Mesothelin Shedding. *Cancer Res* 2011;71:5915–22.
19 Hilliard TS, Kowalski B, Iwamoto K, *et al*. Host Mesothelin Expression Increases Ovarian Cancer Metastasis in the Peritoneal Microenvironment. *Int J Mol Sci* 2021;22:12443.
20 Bütikofer P, Malherbe T, Boschung M, *et al*. GPI-anchored proteins: now you see 'em, now you don't. *FASEB J* 2001;15:545–8.
21 Chowdhury PS, Viner JL, Beers R, *et al*. Isolation of a high-affinity stable single-chain Fv specific for mesothelin from DNA-immunized mice by phage display and construction of a recombinant immunotoxin with anti-tumor activity. *Proc Natl Acad Sci U S A* 1998;95:669–74.
22 Ho M, Feng M, Fisher RJ, *et al*. A novel high-affinity human monoclonal antibody to mesothelin. *Int J Cancer* 2011;128:2020–30.
23 Haas AR, Golden RJ, Litzky LA, *et al*. Two cases of severe pulmonary toxicity from highly active mesothelin-directed CAR T cells. *Mol Ther* 2023;31:2309–25.
24 Liu X, Onda M, Watson N, *et al*. Highly active CAR T cells that bind to a juxtamembrane region of mesothelin and are not blocked by shed mesothelin. *Proc Natl Acad Sci USA* 2022;119.
25 Tang Z, Feng M, Gao W, *et al*. A human single-domain antibody elicits potent antitumor activity by targeting an epitope in mesothelin close to the cancer cell surface. *Mol Cancer Ther* 2013;12:416–26.
26 Golfier S, Kopitz C, Kahnert A, *et al*. Anetumab ravtansine: a novel mesothelin-targeting antibody-drug conjugate cures tumors with heterogeneous target expression favored by bystander effect. *Mol Cancer Ther* 2014;13:1537–48.
27 Lanitis E, Poussin M, Hagemann IS, *et al*. Redirected antitumor activity of primary human lymphocytes transduced with a fully human anti-mesothelin chimeric receptor. *Mol Ther* 2012;20:633–43.
28 Hollevoet K, Mason-Osann E, Liu X, *et al*. In vitro and in vivo activity of the low-immunogenic antimesothelin immunotoxin RG7787 in pancreatic cancer. *Mol Cancer Ther* 2014;13:2040–9.
29 Molloy ME, Austin RJ, Lemon BD, *et al*. Preclinical Characterization of HPN536, a Trispecific, T-Cell-Activating Protein Construct for the Treatment of Mesothelin-Expressing Solid Tumors. *Clin Cancer Res* 2021;27:1452–62.
30 Jiang J, Li S, Tang N, *et al*. Preclinical safety profile of RC88-ADC：a novel mesothelin-targeted antibody conjugated with Monomethyl auristatin E. *Drug Chem Toxicol* 2023;46:24–34.
31 Lin I, Rupert PB, Pilat K, *et al*. Novel mesothelin antibodies enable crystallography of the intact mesothelin ectodomain and engineering of potent, T cell-engaging bispecific therapeutics. *Front Drug Discov* 2023;3.
32 Fierle JK, Abram-Saliba J, Atsaves V, *et al*. A cell-based phenotypic library selection and screening approach for the de novo discovery of novel functional chimeric antigen receptors. *Sci Rep* 2022;12:1136.
33 Hassan R, Butler M, O'Cearbhaill RE, *et al*. Mesothelin-targeting T cell receptor fusion construct cell therapy in refractory solid tumors: phase 1/2 trial interim results. *Nat Med* 2023;29:2099–109.
34 Gaucheron F. The minerals of milk. *Reprod Nutr Dev* 2005;45:473–83.
35 Oyane A, Kim H-M, Furuya T, *et al*. Preparation and assessment of revised simulated body fluids. *J Biomed Mater Res A* 2003;65:188–95.
36 Smyth MJ, Krasovskis E, Johnstone RW. Fas ligand-mediated lysis of self bystander targets by human papillomavirus-specific CD8+ cytotoxic T lymphocytes. *J Virol* 1998;72:5948–54.
37 Klampatsa A, Leibowitz MS, Sun J, *et al*. Analysis and Augmentation of the Immunologic Bystander Effects of CAR T Cell Therapy in a Syngeneic Mouse Cancer Model. *Mol Ther Oncolytics* 2020;18:360–71.
38 Watanabe K, Luo Y, Da T, *et al*. Pancreatic cancer therapy with combined mesothelin-redirected chimeric antigen receptor T cells and cytokine-armed oncolytic adenoviruses. *JCI Insight* 2018;3:e99573.
39 Wang X, Chang W-C, Wong CW, *et al*. A transgene-encoded cell surface polypeptide for selection, in vivo tracking, and ablation of engineered cells. *Blood* 2011;118:1255–63.
40 Hironiwa N, Ishii S, Kadono S, *et al*. Calcium-dependent antigen binding as a novel modality for antibody recycling by endosomal antigen dissociation. *MAbs* 2016;8:65–73.
41 Stearns DJ, Kurosawa S, Sims PJ, *et al*. The interaction of a Ca2+-dependent monoclonal antibody with the protein C activation peptide region. Evidence for obligatory Ca2+ binding to both antigen and antibody. *J Biol Chem* 1988;263:826–32.
42 Zhou T, Hamer DH, Hendrickson WA, *et al*. Interfacial metal and antibody recognition. *Proc Natl Acad Sci U S A* 2005;102:14575–80.
43 Bonifant CL, Szoor A, Torres D, *et al*. CD123-Engager T Cells as a Novel Immunotherapeutic for Acute Myeloid Leukemia. *Mol Ther* 2016;24:1615–26.
44 Choi BD, Yu X, Castano AP, *et al*. CAR-T cells secreting BiTEs circumvent antigen escape without detectable toxicity. *Nat Biotechnol* 2019;37:1049–58.
45 Iwahori K, Kakarla S, Velasquez MP, *et al*. Engager T cells: a new class of antigen-specific T cells that redirect bystander T cells. *Mol Ther* 2015;23:171–8.
46 McGray AJR, Chiello JL, Tsuji T, *et al*. BiTE secretion by adoptively transferred stem-like T cells improves FRα+ ovarian cancer control. *J Immunother Cancer* 2023;11:e006863.
47 Wehrli M, Guinn S, Birocchi F, *et al*. Mesothelin CAR T Cells Secreting Anti-FAP/Anti-CD3 Molecules Efficiently Target Pancreatic Adenocarcinoma and its Stroma. *Clin Cancer Res* 2024;30:1859–77.
48 Yin Y, Rodriguez JL, Li N, *et al*. Locally secreted BiTEs complement CAR T cells by enhancing killing of antigen heterogeneous solid tumors. *Mol Ther* 2022;30:2537–53.
49 Choi BD, Gerstner ER, Frigault MJ, *et al*. Intraventricular CARv3-TEAM-E T Cells in Recurrent Glioblastoma. *N Engl J Med* 2024;390:1290–8.
50 Urbino I, Lengliné E, Valade S, *et al*. Life-threatening complications and intensive care unit management in patients treated with blinatumomab for B-cell acute lymphoblastic leukemia. *Crit Care* 2024;28:14.